Infrared Detector Technology

TNL-TCAD Software

TNL

Technology of Next Level
driven through innovation

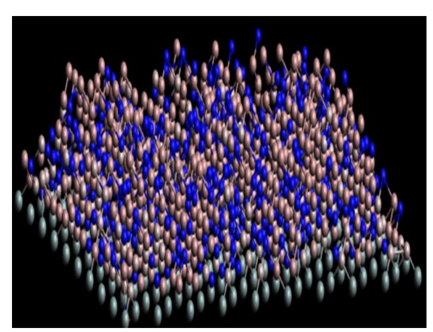

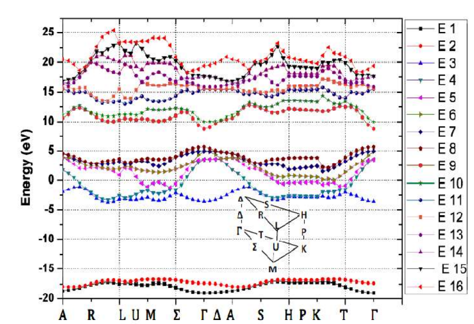

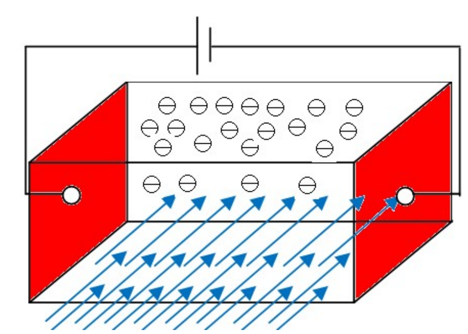

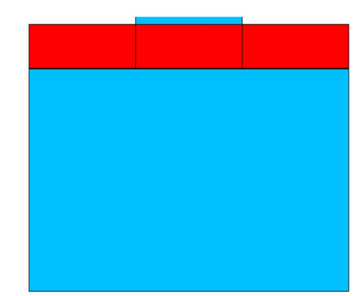

IR DETECTOR/SOURCE TECHNOLOGY

- In 1800, Sir William Herschel discovered the Infrared region of the electromagnetic spectrum, wavelengths spanning from 1 to 75 µm.
- All objects radiate infrared energy above absolute zero temperature is universal fact
- The strong IR absorption through water and atmosphere, make it suitable chioce for sensors and detectors systems and sources, as these radiations are transparent to haze and certain pollutants.
- Used in military as well as civilian applications in thermal imaging, guided missile, reconnaissance, surveillance, ranging and communication systems, space etc.

IR Detector/Source Technology

- *SWIR (1-2µm):* low attenuation Losses for fibre optical communication and is suitable for long distance telecommunications and used to detect the bright plumes of boosting missiles.
- *MWIR (3-5µm):* The guided missile technology, IR imaging system, remote sensing and optical sensors applications exploit the MWIR atmospheric window.
- *LWIR (8–14 µm):* This window can be exploited for free space optical communication at 9.6µm and 10.6µm and thermal imaging applications.
- *VLWIR (beyond 14 µm)* : The VLWIR absorption band is used in astronomical and space applications.

IR Detector/Source Technology

Dominant Materials used in MW- and LWIR Photodetectors are;

- III-V (InAsSb, InGaAs etc) based materials: Mostly used in photovoltaic mode in MIR window, Slow response speed, Technological problem, requires cryogenic cooling
- II-VI (HgCdTe): Dominant infrared detector materials for MIR & LWIR, mostly used in photo-conductive and photovoltaic mode, high sensitive, mature technology, 1/f noise problems reduced, requires cryogenic cooling

CHALLENGES: IR DETECTOR

III–V and II-VI Infrared Detectors

- *Achieving high-efficiency IR detector* and *at the same time driving down the detector cost*
- Materials Used : Group III-V Arsenides and Antimonides, and II-VI (HgCdTe)
- MCT, dominant infrared detector material for MIR & LWIR
- CdZnTe substrate is ideal for epitaxial growth of high performance HgCdTe infrared focal plane arrays (IRFPAs) due to almost zero lattice mismatch
- CZT suffers with serious limitations such as small wafer size, high cost, relatively poor quality, low mechanical strength, and low thermal conductivity
- Cryogenic cooling (77 K) in order to reduce noise and leakage currents
- Two main epitaxial growth techniques: liquid-phase epitaxy (LPE); and vapor-phase epitaxy (VPE)

IR Detector Technology

- VPE techniques, molecular beam epitaxy (MBE) and metal–organic chemical vapor deposition (MOCVD) allow the construction of more complex device structures *with other substrates R & D options*, with good lateral homogeneity and abrupt composition and doping profiles
- However, lattice and thermal mismatch is important due to industry trend towards smaller pixel size and larger detector arrays
- Stress due to lattice and thermal mismatch in epitaxially-grown semiconductors leads to mismatch defects (dislocations), have impact on yield and electro-optical properties of the device
- Large lattice mismatch between HgCdTe and the alternative substrates, a large dislocation density is observed, reduces the performance of HgCdTe IR detectors

Design Criteria & Challenges

Key approaches for MCT Growth over other substrates (Si, Ge, GaAs, GaSb, CZT)

(i) MBE Reactor growth: ***promising path, require buffer, with several challenges e.g. growth rate, lattice mismatch, strain, types of defect generation***

(ii) MOCVD Reactor growth: ***Realize novel detector designs through multilayer in situ growth, with complete flexibility in choice of alloy compositions and doping concentrations favoring HOT conditions***

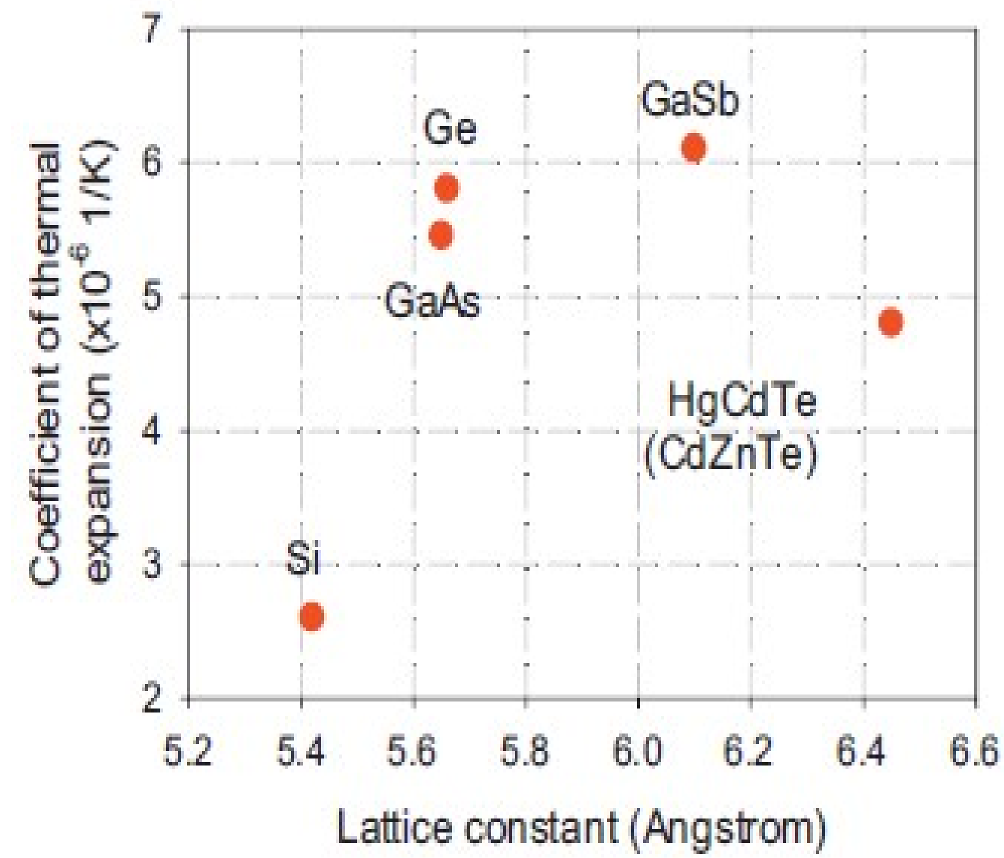

* http://dx.doi.org/10.1016/j.jcrysgro.2016.12.034

Heteroepitaxy: Challenges

- Band gaps Tuning : Depends on material thickness, composition, defects etc
- Efficient absorption: Depends on thickness of active region
- High thermal/chemical stability: allow operations in extreme conditions in space
- lattice-mismatch: Epitaxy of HgCdTe on Si, Ge, GaAs extremely challenging
- Formation of defects and dislocations due to strain
- Such defects limit detector performance

Substrate	Si	GaAs	GaSb	Ge	CZT	CdTe
Lattice Mismatch(%)	19	14	6	15	~0	0.3

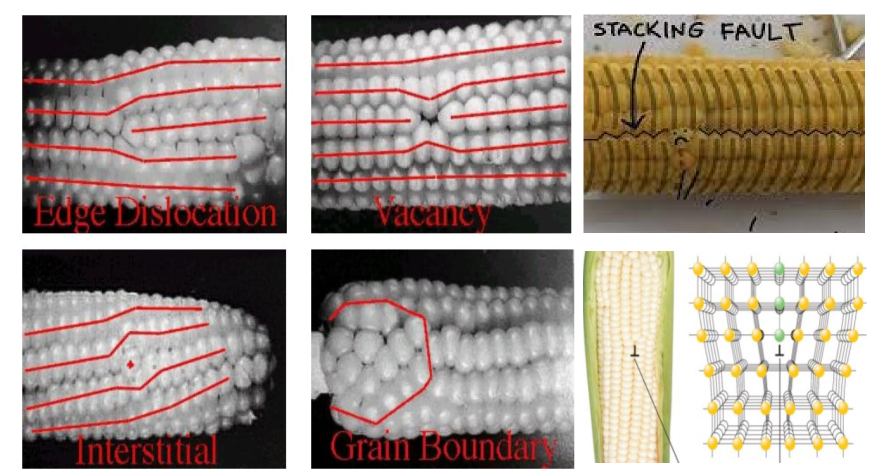

Solutions: Hetero-Epitaxy

- MCT-on-Si detector recently attracted much attention due due to *cost & large size Si substrates availability* with possibility *of co-processing in CMOS foundries*
- Huge investment require for ***Hits and Trails***
- ***Reduce waste***
- Understanding of behaviors of parasitic interfaces at multiple junctions: *crucial to reduce the losses*
- ***To save the design cost and development time, use of TNL-computer-aided design (TNL-CAD) tools at atomistic scale will make the difference***
- ***TNL-MOCVD and TNL-MBE reactor's based epitaxial growth processes to replicate real time growth experiments with Process Optimization Facilities.***

TNL - Epitaxy Process Solution

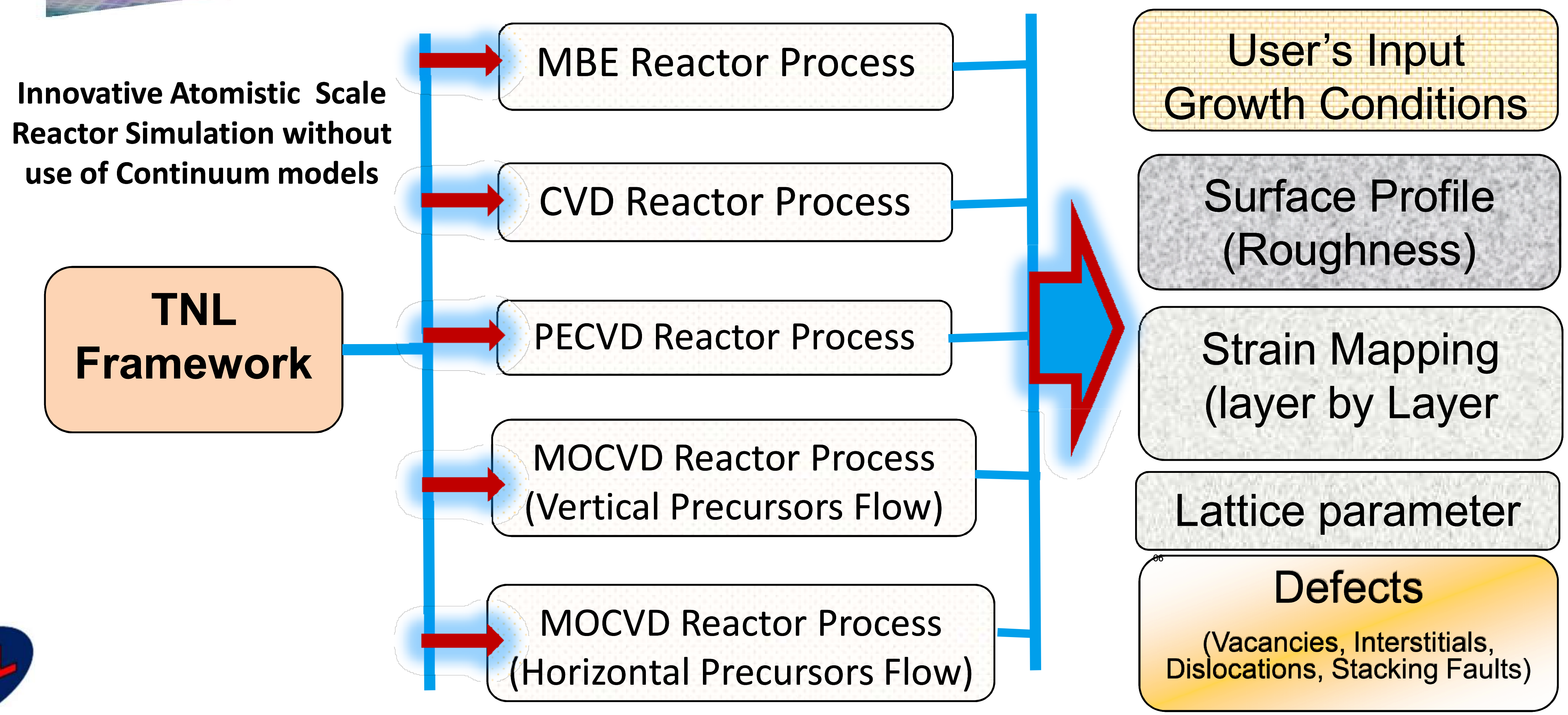

Inputs : MOCVD Process

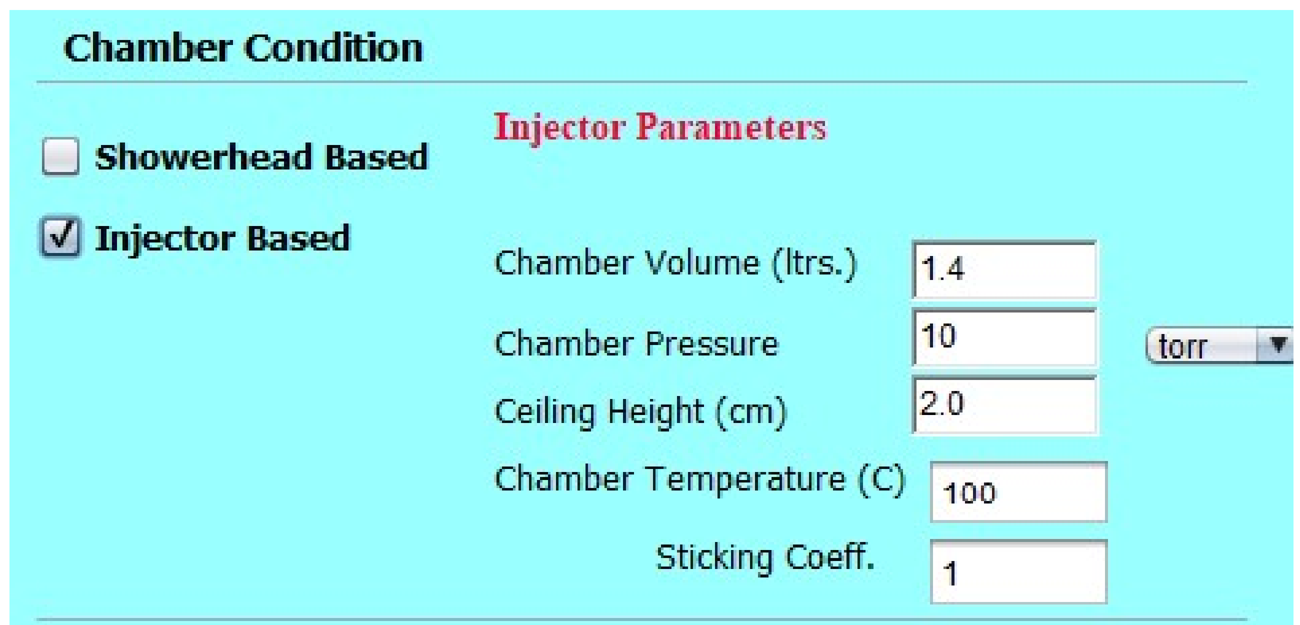

Many More parameters details Require ……….

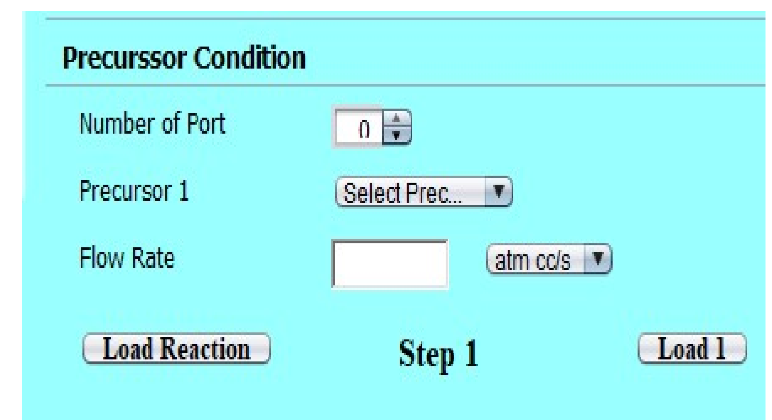

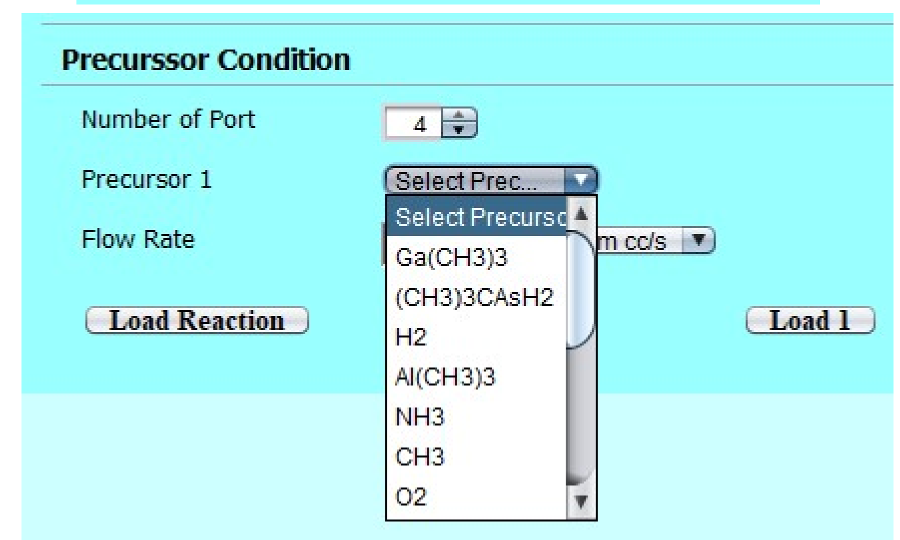

Methodology: MOCVD Process

Schwoebel barrier: The atom diffuses from the site exactly above the edge atom to the site immediately next to the edge atom as;

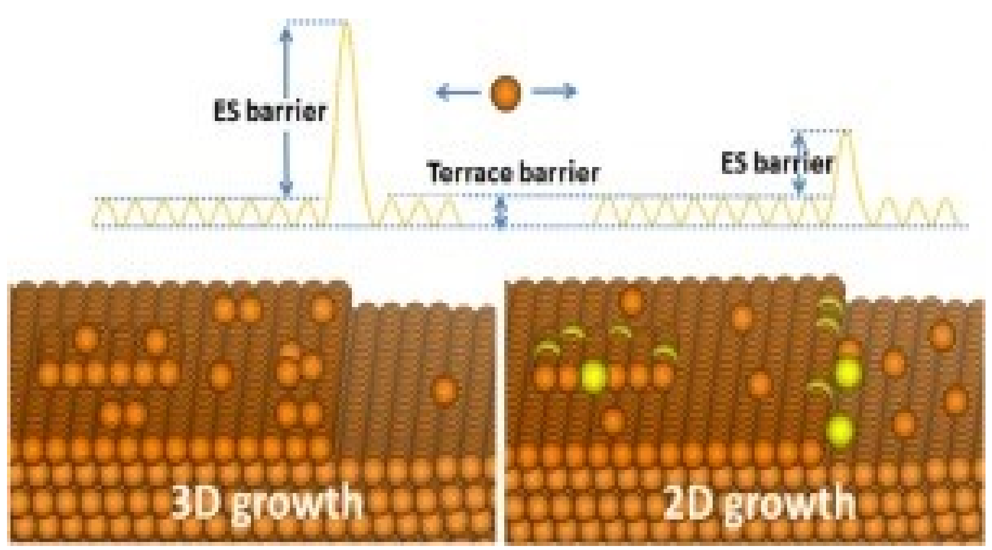

Incorporation barrier: The atom incorporates into the edge on the same surface level.

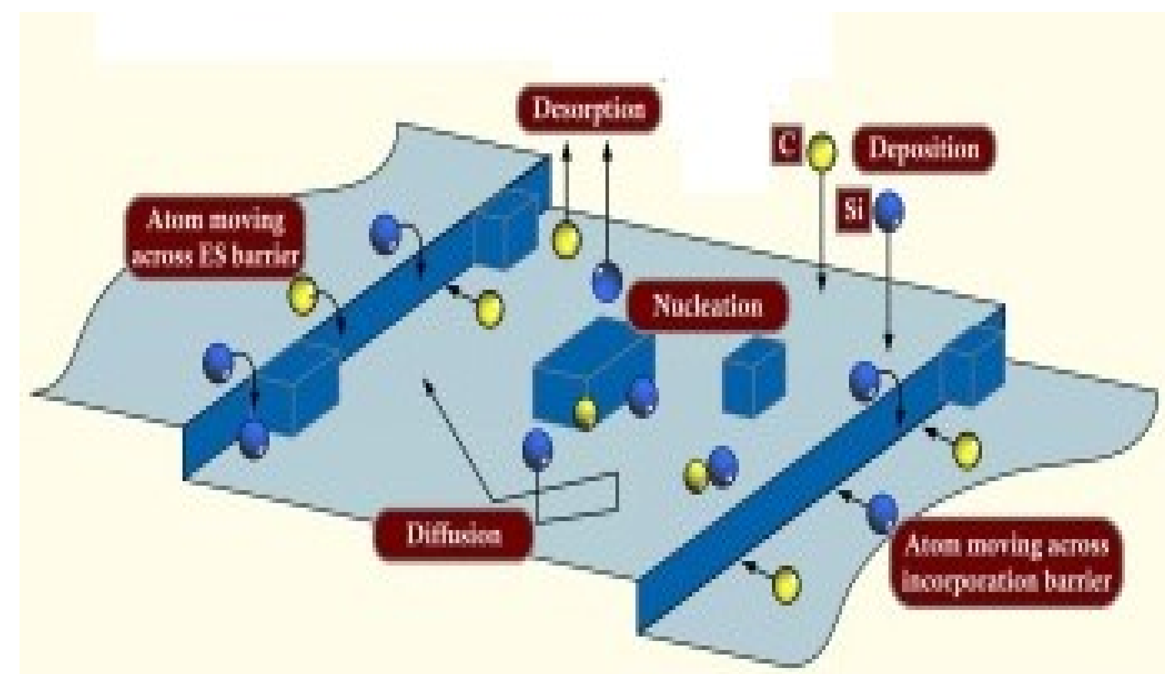

PLANETARY MOCVD PROCESS

Planetary MOCVD architecture implemented in ***TNL-Injector* simulator** equivalent to the **AIX 200/4 horizontal MOCVD reactor**.

Inlet of the reactor is divided into two parts by a separator through which the group II and VI precursors can be fed into the upper and lower inlet respectively.

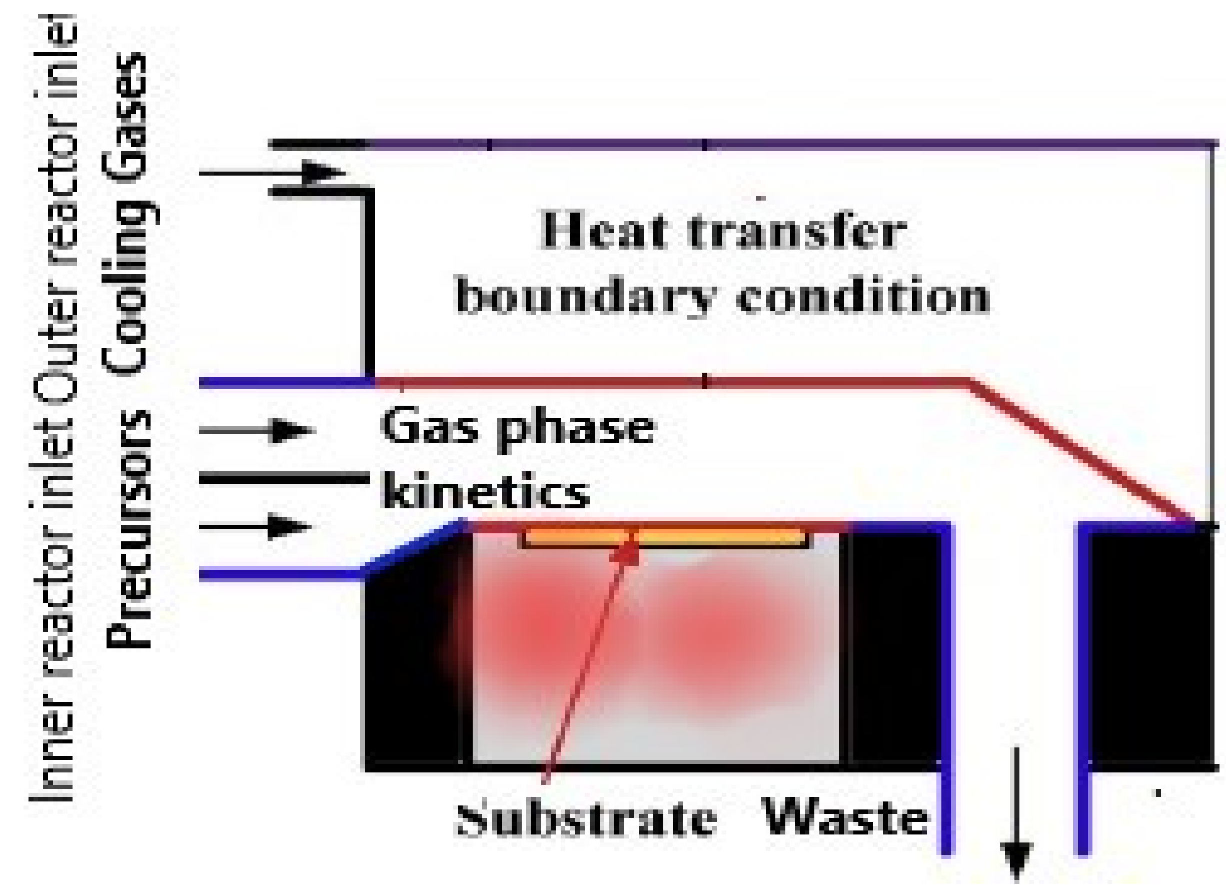

PLANETARY MOCVD PROCESS

The reactant flux, $J_A = -\frac{D_{AB}}{RT}\frac{dc_A}{dx}$ with $\frac{dc_A}{dx} \approx \frac{\Delta c_A}{\Delta x} = \frac{c_{AB} - c_{AS}}{\delta}$

where J_A is the diffusion flux of specie A, is the concentration of species A, x is the direction perpendicular to the substrate surface, *R* is the gas constant, *T* is the absolutc$_A$ e temperature. δ is the chamber boundary layer thickness.

D_{A_B} is the diffusivity of the bulk stream reactants and dependent on Leonard-Jones parameters (σ, Ω) based on the Chapman-Enskog theory

$$D_{A_B} = 2.7 \times 10^{-3} \frac{\sqrt{T^3\left(\frac{1}{M_A}+\frac{1}{M_B}\right)}}{p\,\sigma_{AB}^2\,\Omega_{D,AB}}$$

M is the molecular weight, p is the pressure, σ_{AB} is the collision diameter, and Ω_D, AB is the collision integral and dependent on temperature and intermolecular potential.

Average boundary layer thickness, δ, $\bar{\delta} = \frac{10}{3}\sqrt{\frac{\mu_{mix} L}{\rho U}}$

Planetary MOCVD Process

An Injector MOCVD reaction initiate either surface kinetic or mass transport control. Suppose C_g is the concentration of the bulk gas and C_s is the concentration of reactants at the substrate interface. The concentration of the reactants drops from the bulk to the substrate surface and the corresponding mass flux,

$$J_{gs} = h_g(C_g - C_s)$$

where h_g is the gas mass transfer coefficient, insensitive to variations in temperature.

The flux consumed at the surface $J_s = k_s(C_s)$ where $C_s = \frac{C_g}{1+\frac{k_s}{h_g}}$

where k_s is the slowest surface reaction rate constant.

For $\boldsymbol{k_s >> h_g}$, the system dictated by mass controlled , low gas transport rate through the boundary layer limits the rapid surface reaction.

Surface reaction control dominates for $\boldsymbol{h_g >> k_s}$, the surface reaction is slow even through sufficient reactant gas is available. Additionally, h_g increases with increasing pressure and decreasing temperature and k_s follows the Arrhenius equation.

Working

- Gas phase kinetics
- Surface phase kinetics
- Each monolayer with atoms positions
- Defects layer by layer quantitatively and qualitatively
- Strain layer by layer
- Surface Roughness
- Lattice Constant etc.

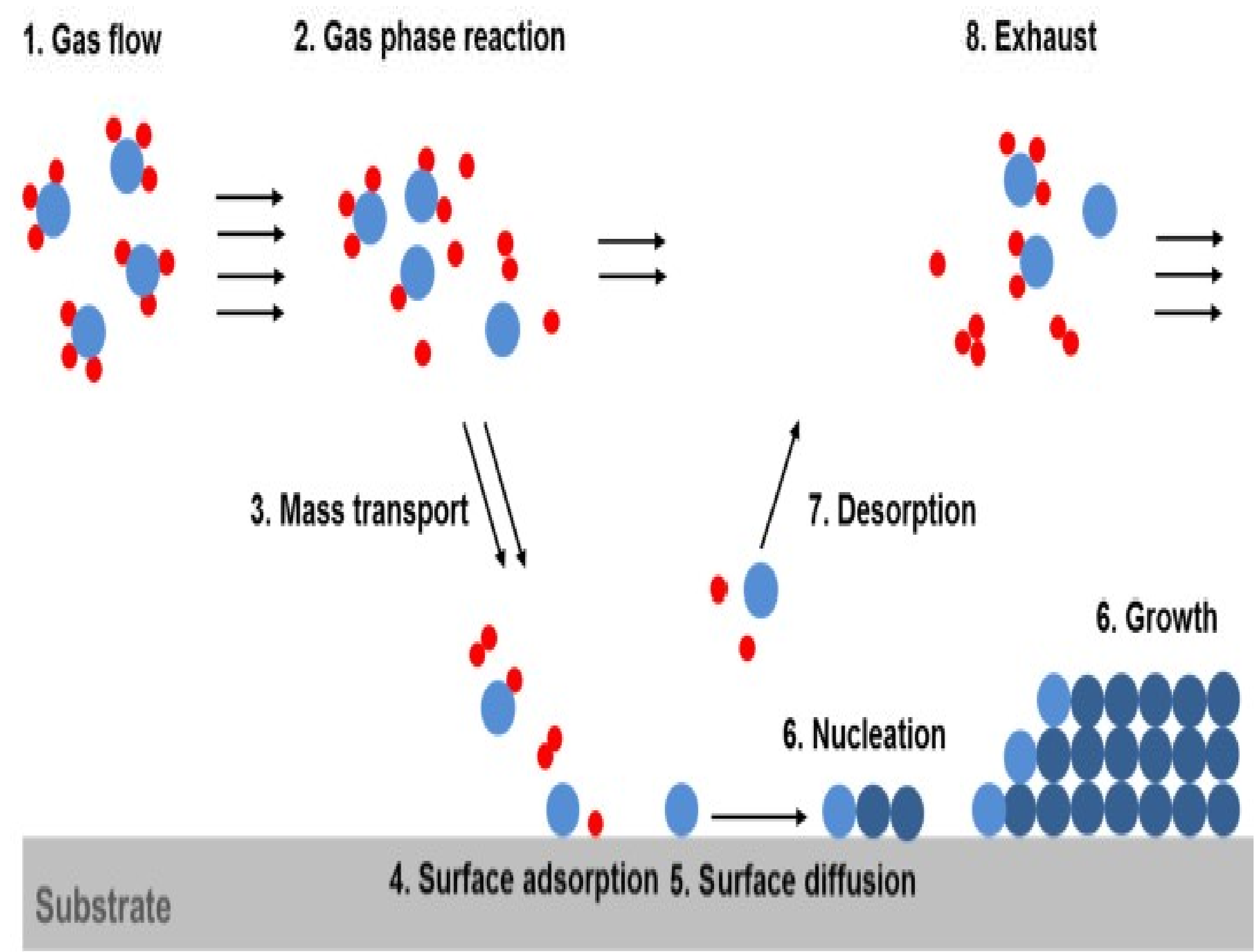

Chemical Kinetics Solution

- TNL Chemical Kinetics database includes gas- and surface phase chemical reactions
- Users may chose any desired equation or set of equations for the precursors they input based on requirements
- Users have flexibilities to write their own chemical reactions

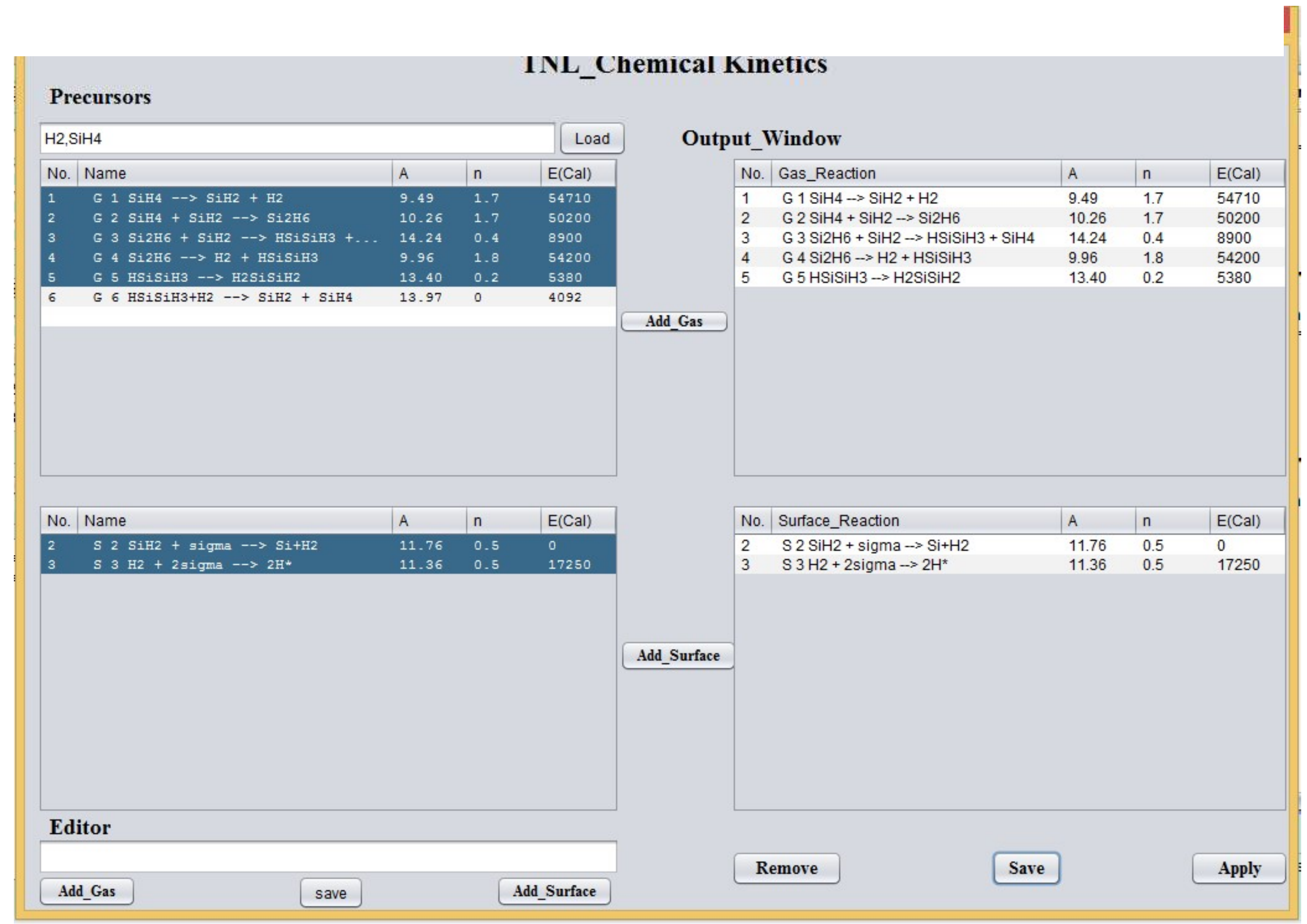

TNL

TNL Chemical Database

Precursors for MCT Growth

Dimethylcadmium (DMCd), $Cd(CH_3)_2$, $Te(CH_3)_2$, diisopropyl telluride (DIPTe), vapor of Hg

Dopants

Ethyl iodide (EI) and tris-(dimethylamino)arsenic (TDMAAs)

Carrier Gases: H_2 , Ar etc.

$$A + B \leftrightarrow AB$$

$$\frac{d[AB]}{dt} = \frac{k_1[A][B]^2}{1 + k_2[A] + k_3[B]^{1/2}}$$

Reaction rates in forward and reverse directions

$$k = AT^n \exp\left(-\frac{E_a}{RT}\right)$$

CHEMICAL KINETICS

Gas Phase Reactions

	Reaction	$Log_{10}A$	α	E_a/R	ΔH_r (kJ/mol)
Q1	$Cd(CH_3)_2 + H \rightarrow CdCH_3 + CH_4$	14.5	0	3150	−213.5
Q2	$Te(CH_3)_2 + H \rightarrow TeCH_3 + CH_4$	13.8	0	3750	−209.3
Q3	$Cd(CH_3)_2 + CH_3 \rightarrow CdCH_3 + C_2H_6$	12.9	0	8450	−128.5
Q4	$Te(CH_3)_2 + CH_3 \rightarrow TeCH_3 + C_2H_6$	11.1	0	7550	−123.5
Q5	$Te(CH_3)_2 + CdCH_3 \rightarrow CH_3TeCd + C_2H_6$	10.8	0	12550	−136.6
Q6	$Te(CH_3)_2 + Cd(CH_3)_2 \rightarrow CH_3TeCd\,CH_3 + C_2H_6$	10.1	0	28500	−126.1

Surface Phase Reactions

	Reaction	$Log_{10}A$	α	E_a/R
S1	$Cd(CH_3)_2 + \sigma \rightarrow [Cd(CH_3)_2]_{ads}$	9.6	0.5	0
S2	$CdCH_3 + \sigma \rightarrow [CdCH_3]_{ads}$	11.6	0.5	0
S3	$[Cd(CH_3)_2]_{ads} \rightarrow [CdCH_3]_{ads} + CH_3$	16.0	0	16500
S4	$[Cd(CH_3)_2]_{ads} \rightarrow Cd(CH_3)_2 + \sigma$	11.0	0	5000
S5	$CH_3 + [CdCH_3]_{ads} \rightarrow [Cd(CH_3)_2]_{ads}$	9.1	0.5	0
S6	$Te(CH_3)_2 + [CdCH_3]_{ads} \rightarrow [CdTeCH_3]_{ads} + C_2H_6$	18.0	0	13500
S7	$[CdTeCH_3]_{ads} \rightarrow CdTe_{film} + CH_3 + \sigma$	12.0	0	12500
S8	$TeCH_3 + [CdCH_3]_{ads} \rightarrow CdTe_{film} + 2CH_3 + \sigma$	18.0	0	10000

Assuming Hg vapor flux is direct to the substrate surface

METHODOLOGY: KMC

Total Deposition Rate:

$$R = A + H + D$$

A - Adsorption, H – Diffusion, D - Desorption rates

$$A = Flw$$

Here, l and w denote length and width of substrate

$$h_j = D_0 exp\left(-\frac{E_j}{k_B T}\right)$$

The characteristic vibration frequency , $D_0 = \frac{2k_B T}{h}$

$$d_j = D_0 exp\left(-\frac{E_j^{des}}{k_B T}\right)$$

with $E_j^{des} = E_S + nE_n$

EXTRACTABLE

1. Lattice Parameters:

- ❑ Layer by layer lattice parameter Extraction.
- ❑ Averaging layer by layer lattice constant may produce overall lattice constant of film.
- ❑ The lattice constant can be calibrated with lattice constant with XRD studies.
- ❑ Lattice constant includes all the strain, defects etc effects.

2. Strain:

- ❑ Averaging layer by layer strain produce overall strain in the film.
- ❑ The strain can be calibrated with experimental strain.

3. Surface Roughness:

- ❑ Extract surface roughness as a function of growth time

$$r = \sqrt{\frac{\sum_{i=1}^{N}\sum_{j=1}^{N}[h_{ij}-\bar{h}]^2}{NxN}}$$

Here N is the total number of lattice points, h_{ij} is the height at a given lattice point located at position *i* and *j*, on the lattice and h_{avg} is the average height of all lattice points.

4. Mole fraction:

- ❑ Extract number of atoms of different constituents layer by layer.
- ❑ Ratio of group-III & V deposited atoms ➡ Molefraction.

5. Defects :

- ❑ Extract number of interstitials, vacancy etc layer by layer along with dislocation and Stacking Faults

CASE STUDY: MBE GROWTH $Hg_{1-x}Cd_xTe$ ON GaAs, GaSb, CZT SUBSTRATES

Input Conditions

Substrate	Lattice Constant	Substrate (unitcells^2)	Sub. Temp.	Effusion Cell Cd	Effusion Cell Hg	Effusion Cell Te	Time	Process Steps
GaAs	5.65 A	30x30	200^{o}C	200^{o}C	35^{o}C	200^{o}C	50s each Step	2 Steps; CdTe & MCT
GaSb	6.095 A	30x30						2 Steps; CdTe & MCT
CZT	6.468 A	30x30						2 Steps; CdTe & MCT

$$1\ unitcell \times 1\ unitcell = lattice\ constant^2\ \AA^2$$

EXTRACTED OUTPUT PARAMETERS

Parameters		GaAs/CdTe/ HgCdTe		GaSb/CdTe/HgCdTe		CdZnTe/CdTe/HgCdTe	
		CdTe	**HgCdTe**	**CdTe**	**HgCdTe**	**CdTe**	**HgCdTe**
Lattice parameter (°A)	**a**	5.9594	5.9713	6.4495	6.9783	6.1489	6.4765
	b	5.9662	6.6454	6.3471	6.6695	6.0663	6.0995
	c	6.6470	6.4843	6.6167	6.4108	6.1512	5.7141
Total deposited atoms		604755		696705		776608	
Dislocation Density ($/cm^2$) (Ist / IInd Growth Steps)		$CdTe_{dis} = 6.78x10^{11}$ $HgCdTe_{dis} = 2.32x10^{12}$		$CdTe_{dis} = 5.88x10^{11}$ $HgCdTe_{dis} = 2.13x10^{12}$		$CdTe_{dis} = 1.69x10^{11}$ $HgCdTe_{dis} = 1.92x10^{12}$	
Total Vacancies		20%		19%		18%	

OUTPUT

Atomistic arrangement of atoms of deposited CdTe buffer layers over GaAs followed by deposited $Hg_{1-x}Cd_xTe$ atoms.

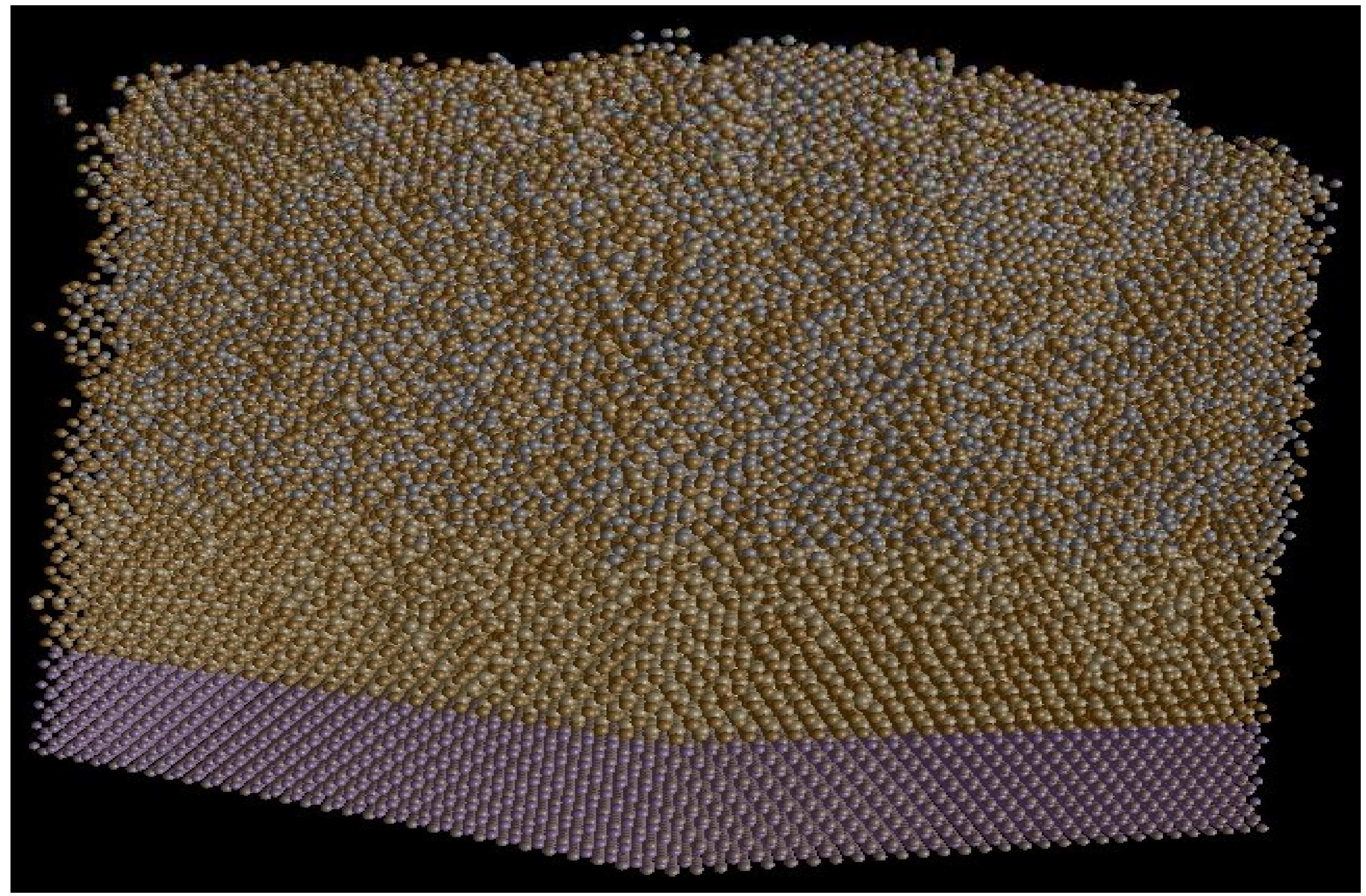

DISLOCATIONS PER MONOLAYER

Dislocation Density within deposited layers over **GaAs** substrate

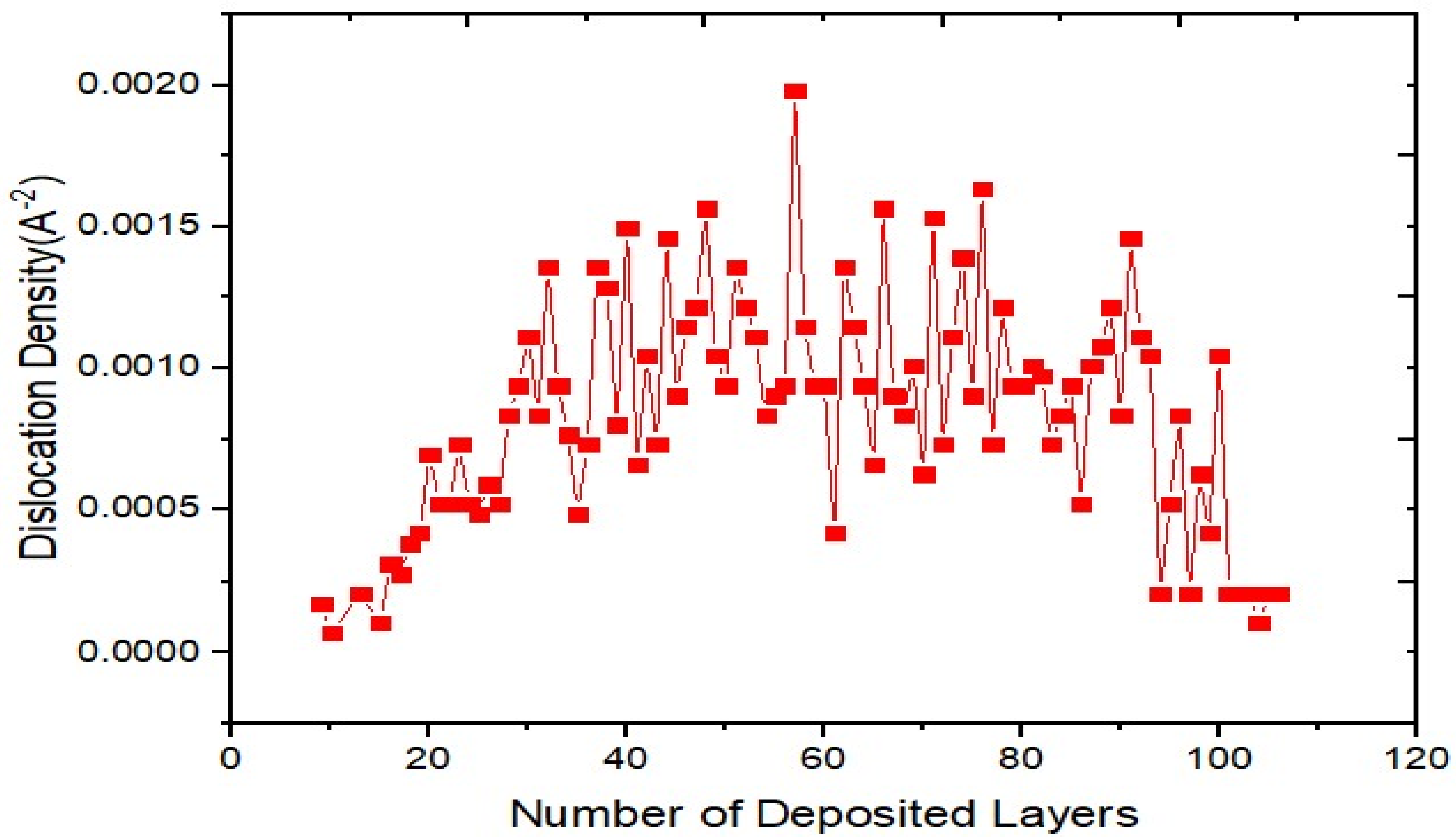

DISLOCATIONS PER MONOLAYER

Dislocation Density within deposited layers over **GaSb** substrate

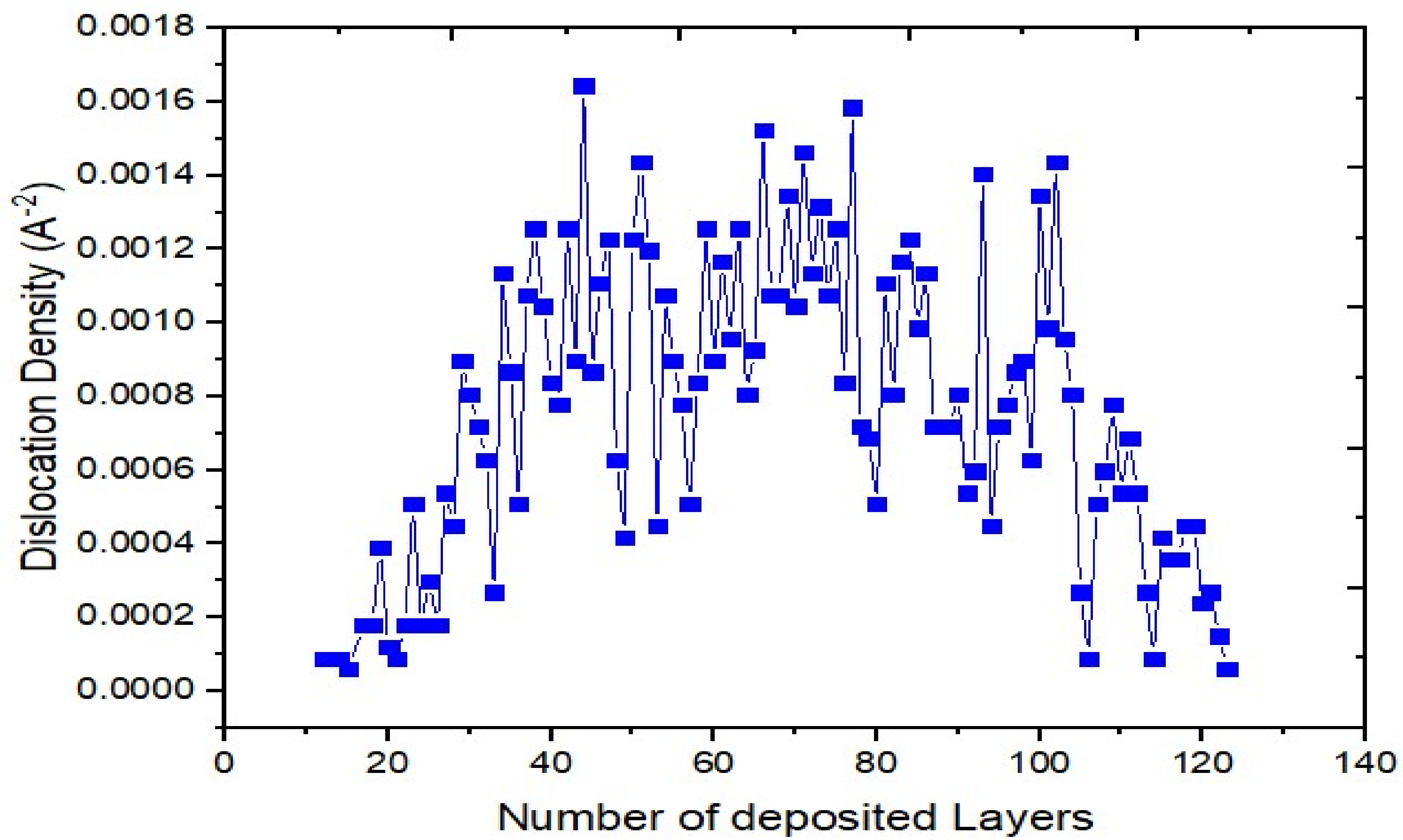

Dislocations per Monolayer

Dislocation Density with deposited layers over **CdZnTe** substrate

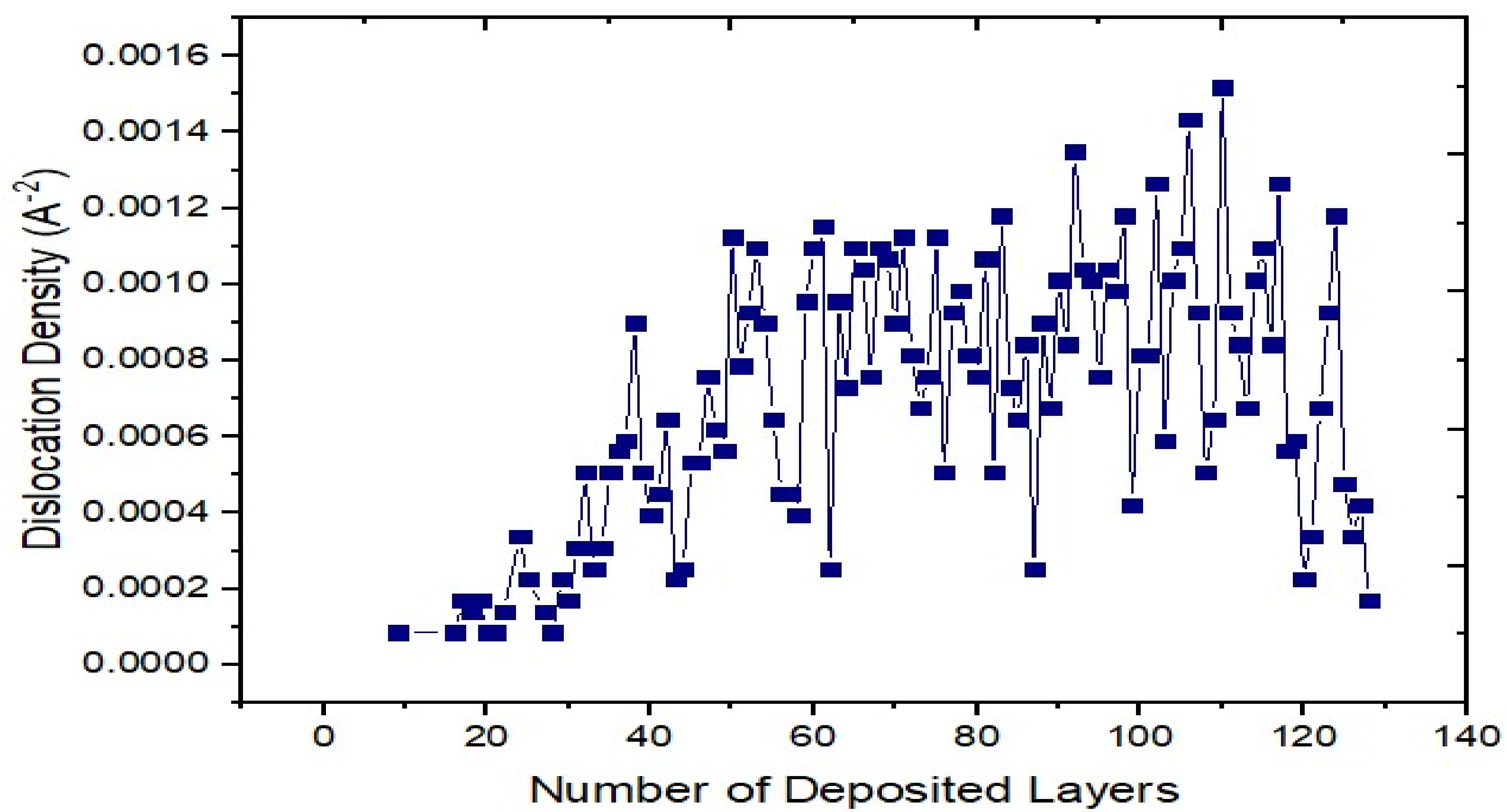

Epitaxy Conclusion

- The *TNL-MBE reactor* proven capabilities to reproduce MCT deposition process as per the real time process experiments.
- The growth rates can be matched with the experimental growth rates.
- On the basis of output results, CZT substrate shown superiority for MCT deposition.
- Bigger size substrates i.e. GaAs and GaSb for MCT growth can be chosen for R & D
- There is still big room to optimize and improve the output results in terms to further reduce the defect densities.
- *TNL-EpiGrow™* simulators are capable to expedite the CVD, Lateral & vertical MOCVD reactors based epitaxial processes development by reducing cost and manpower consumptions. The MBE reactor process can be optimized to achieve high quality MCT films for MW & LW IR detection applications.

InGaAs/InP IR PHOTODETECTOR

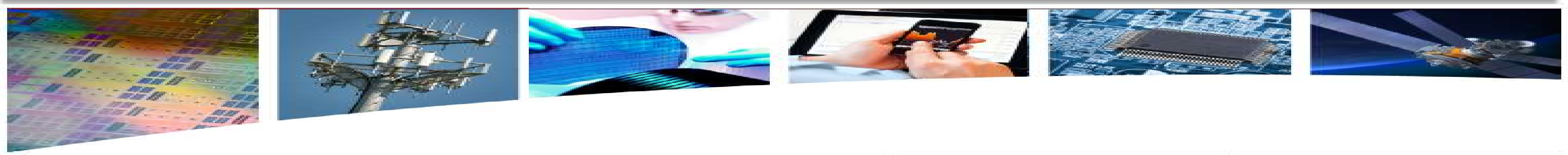

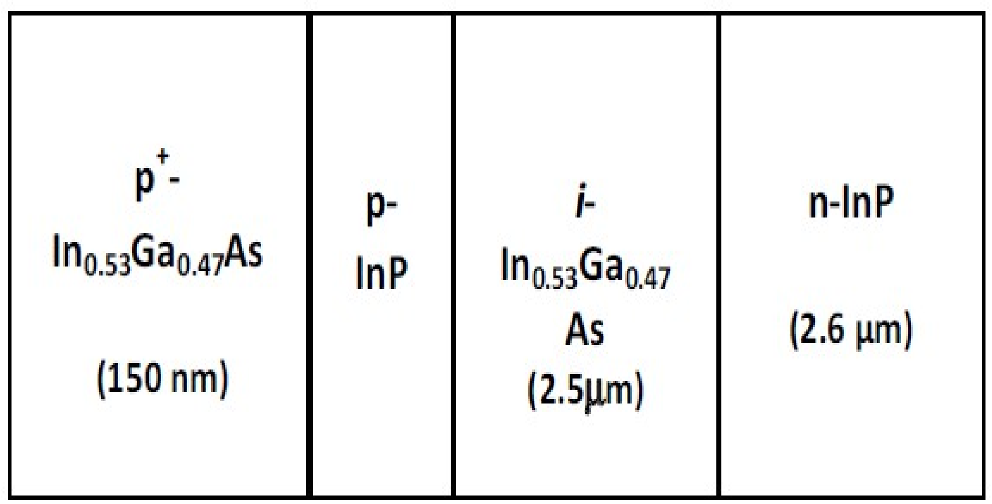

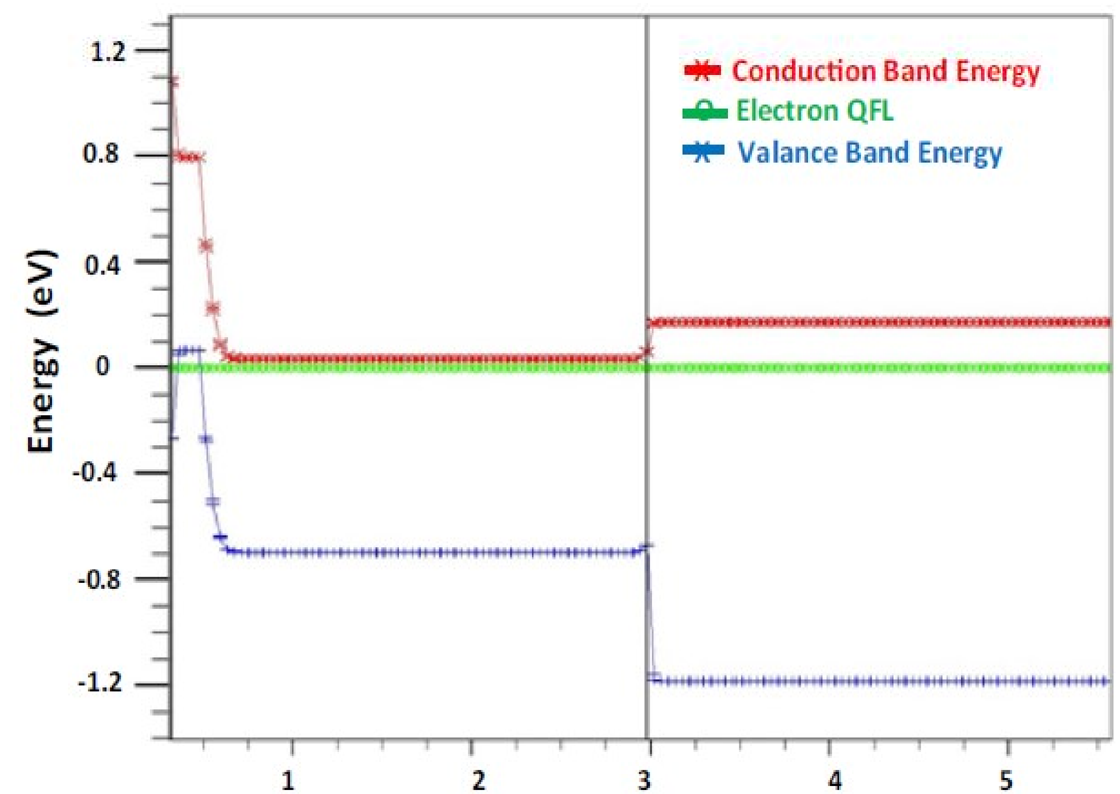

I–V CHARACTERISTICS

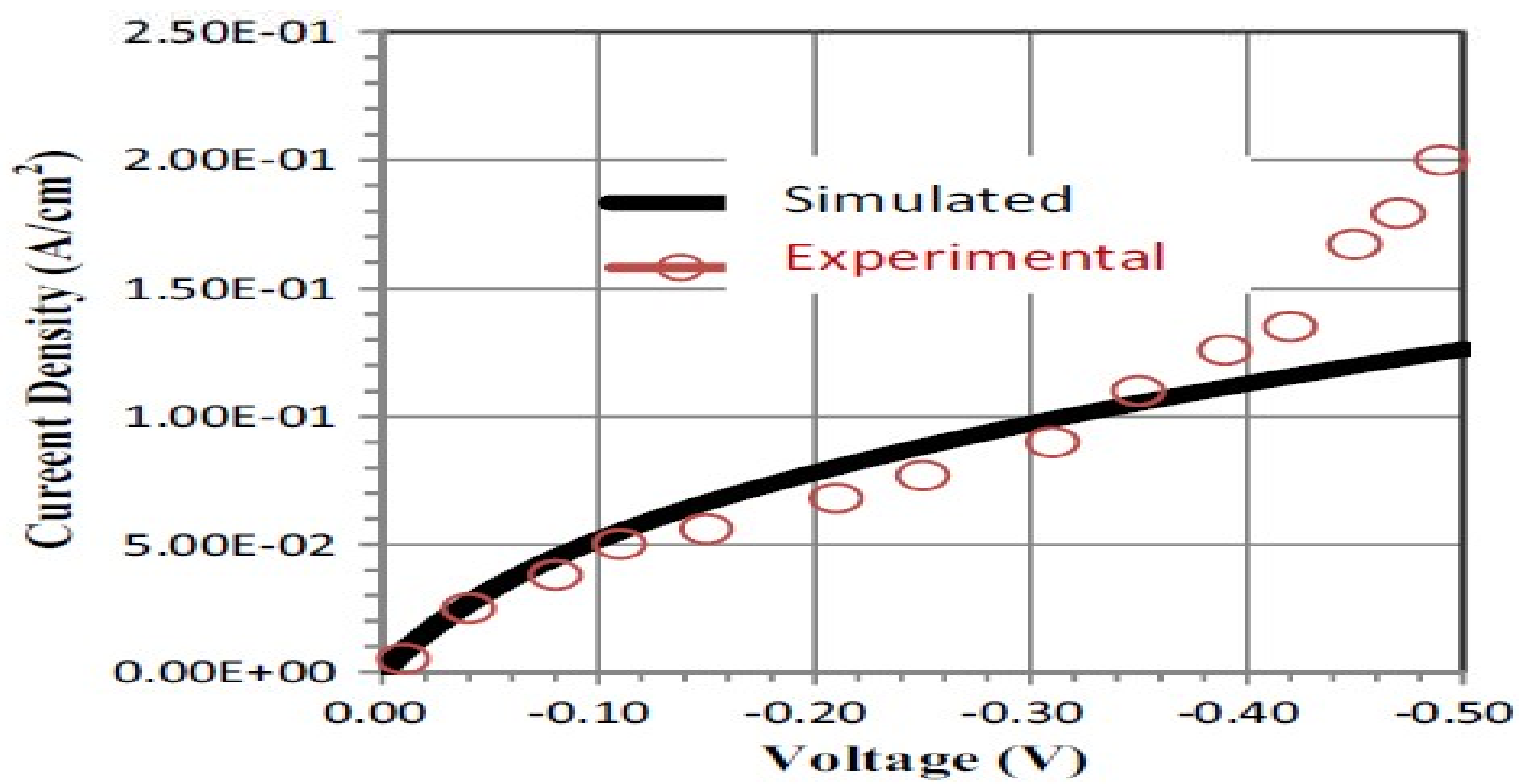

Infrared Detector

Table 1 The current density values for different doping dose at specified absorbing layer thickness

Doping dose (cm^{-3})	Current density at specified absorbing layer thickness (A/cm^2)		
	2 µm	2.5 µm	3 µm
5.1×10^{15}	2.53×10^{-07}	2.53926×10^{-07}	2.54×10^{-07}
1.1×10^{16}	1.62×10^{-07}	1.63×10^{-07}	1.63×10^{-07}
5.1×10^{16}	2.6456×10^{-08}	2.6898×10^{-08}	2.7595×10^{-08}

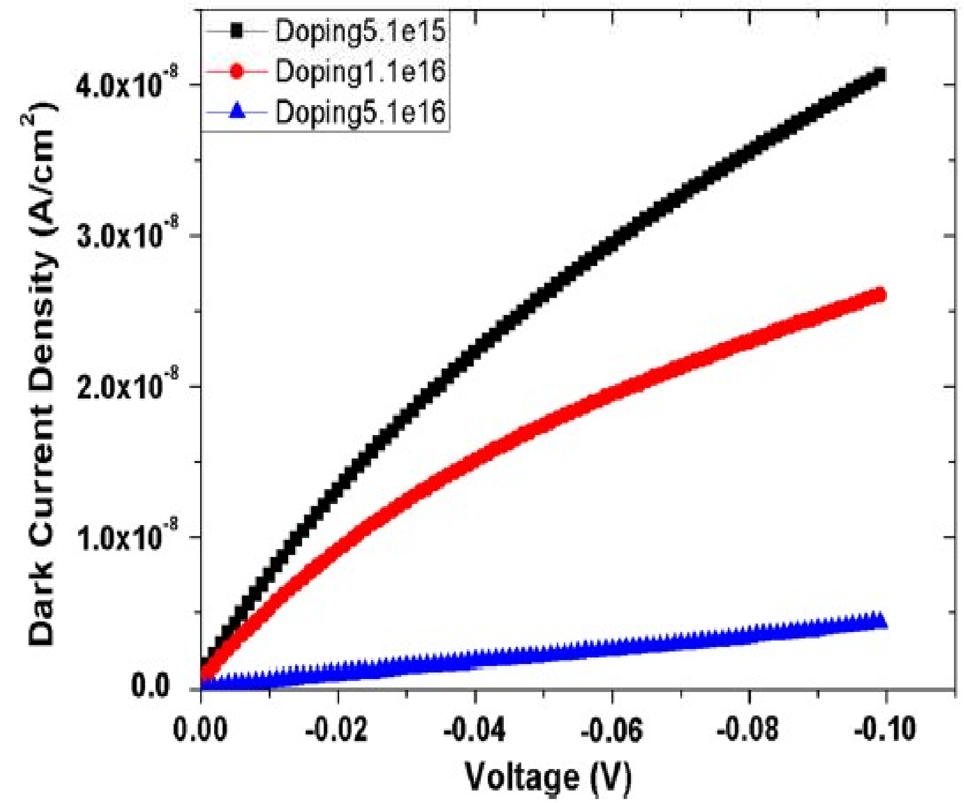

Quantum Efficiency

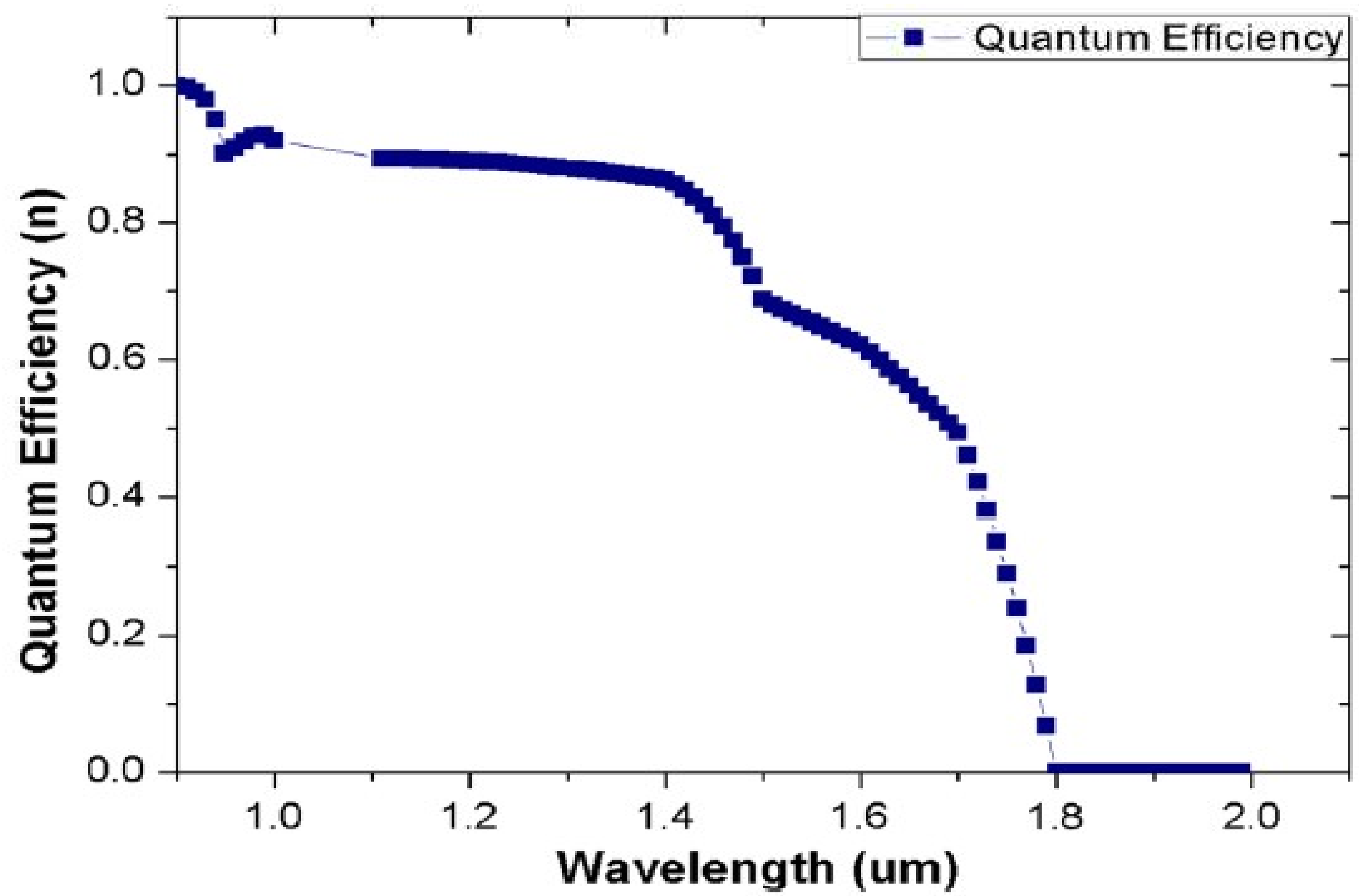

ADVANCE LICENSING & PRICE VALUE

TNL's tools support advanced and unique licensing models tailored for unique customer needs.

➢ ADVANCED LICENSING OPTIONS:

- Term-Based
- Perpetual with Annual Maintenance Cost (AMC)
- TCAD Academic Suite
- 24x7 Technical Support for **Academic Institutions**

Publications

1. P.K. Saxena, numerical study of dual band (MW/LW) ir detector for Performance improvement, *Defence Science Journal*, vol. 67(2), (2017) pp. 141-148. DOI : 10.14429/dsj.67.11177
2. Praveen K. Saxena, Pankaj Srivastava, R. Trigunayat, An innovative approach for controlled epitaxial growth of GaAs in real MOCVD reactor environment, *Journal of Alloys and Compounds, vol.* 809 (2019) 151752. https://doi.org/10.1016/j.jallcom.2019.151752
3. Praveen Saxena, R. Trigunayat, Anchal Srivastava, Pankaj Srivastava, Md. Zain, R.K. Shukla, Nishant Kumar, Shivendra Tripathi, FULL ELECTRONIC BAND STURCTURE ANALYSIS OF Cd DOPED ZnO THIN FILMS DEPOSITED BY SOL-GEL SPIN COATING METHOD , II-VI US Workshop Proceedings, 2019.
4. R. K. Nanda, E. Mohapatra, T. P. Dash, P. Saxena, P. Srivastava, R. Trigutnayat, C. K. Maiti, Atomistic Level Process to Device Simulation of GaNFET Using TNL TCAD Tools, Advances in Electrical Control and Signal Systems pp 815-826, (2020), Spinger Book. https://doi.org/10.1007/978-981-15-5262-5_61
5. Sanjeev Tyagi, P. K. Saxena, Rishabh Kumar, Numerical simulation of InxGa1−xAs/InP PIN photodetector for optimum performance at 298 K, Optical and Quantum Electronics (2020) 52:374. https://doi.org/10.1007/s11082-020-02488-1
6. A. Srivastava, A. Saxena, P. K. Saxena, F. K.Gupta, P. Shakya, P. Srivastava, M. Dixit, S.Gambhir, R. K. Shukla & A. Srivastava, An innovative technique for electronic transport model of group-III nitrides, *Scientific Reports* 10, 18706 (2020).
7. PK Saxena, A Srivastava, A Saxena, F Gupta, P Shakya, A Srivastava, et. al., An Innovative Model for Electronic Band Structure Analysis of Doped and Un-Doped ZnO, Journal of Electronic Materials 50 (4), 2417-2424(2021).
8. P. K. Saxena, F. K. Gupta, A. Srivastava, P. Srivastava1 and Anshu Saxena, Ultrafast carrier's dynamics with scattering rate saturation in Ge thinfilmsUltrafast carrier's dynamics with scattering rate saturation in Ge thinfilms TechRxiv · Mar 17, 2022

Thank You

Contact us

+91-983-915-1284

info@technextlab.com

Lucknow 226 003, INDIA

www.technextlab.com

TNL